

# Evaluation of Fractional-Order Sliding Mode Control Applied to an Energy Harvesting System

Julio Cesar C. Basilio<sup>1</sup>, Tiago Roux Oliveira<sup>2</sup>, José Geraldo T. Ribeiro<sup>3</sup> and Americo Cunha Jr<sup>4</sup>

**Abstract**—The use of fractional operators in control theory is recent and new approaches are emerging more and more. The existing literature shows improvement in control performance when using fractional controllers. One of the main reasons for this improvement is due to the greater number of control parameters, inserted by the exponents that represents the fractional-order of the integral or derivative operators. Another interesting feature of fractional calculus is that it is often used to describe phenomena with memory. In this context, this paper proposes a comparison between Sliding Mode Controls of Integer-Order (SMC) and Fractional-Order (FOSMC). Sliding Mode Control is one of the most successful approaches in dealing with uncertainties and one of the most efficient in nonlinear dynamics. The problem chosen for the application of the controllers is a nonlinear bi-stable vibration energy harvesting system, since controlling this system makes the relationship between generated energy and consumed energy (control effort) very important, being an ideal situation to evaluate and compare the performance of the two methods. A novelty in this paper is the use of the Cross Entropy optimization method to obtain the set of optimal parameters (best performance) in the SMC and FOSMC controllers. The result of the optimization tests reinforces the improvement in the use of the fractional operator reducing the control effort by up to 93% when compared to the integer-order controller. The Cross Entropy method was also very effective for controllers with a large number of adjustment parameters.

## I. INTRODUCTION

Studies on the application of fractional operators in control theory are increasingly in the literature, mainly due to the benefits they provide in control performance. Fractional-order operators are known to describing phenomena with memory. In addition, the exponents of fractional operators in a control system provide a additional degree of freedom for tuning a controller, enabling improvements in the controller performance as well [16].

Several control techniques already have a fractional version, from classical control methods, such as the PID (Proportional-Integral-Derivative) controller [4] [10], to robust control methods, such as the Sliding Mode Control (SMC) [1] [18].

From the fractional method proposed by [1], this paper compares a classic Sliding Mode Control (SMC) and a Fractional-Order Sliding Mode Control (FOSMC), focusing on the performance evaluation of controllers for energy consumption. Thus, the system chosen to be controlled is

a nonlinear bistable vibration energy harvester, precisely because of the importance of the relationship between generated energy and consumed energy. It is worth noting that the study aims to evaluate the performance of the controller and not the feasibility of a controller of this type in this energy harvester. Finally, to obtain the set of optimal parameters (best performance) of the two controllers, the optimization by the Cross-Entropy method is performed. This global optimization method is chosen mainly because it has a good efficiency in problems with many design variables, as is the case with fractional controllers.

## II. ENERGY HARVESTER

Based on the concept of nonlinear vibratory energy harvesting introduced by [7], a bistable piezoelectric energy capture system proposed by [13], represented in Fig. 1, is used in this paper to application and comparison of controllers performance.

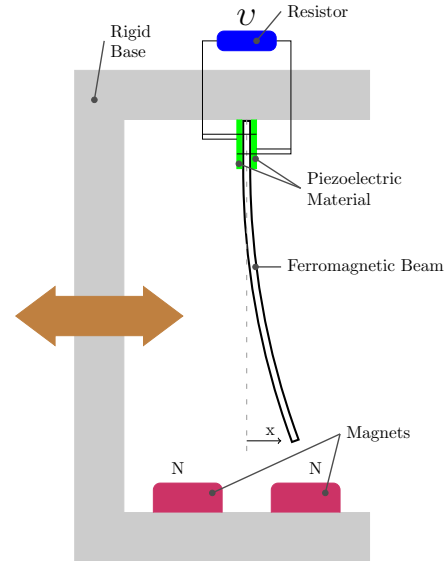


Fig. 1. Schematic representation of a non-linear bistable energy harvester.

The mathematical model of the energy harvester dynamics is represented by the following dimensionless equations

$$\ddot{x} + 2\xi\dot{x} - \frac{1}{2}x(1-x^2) - \chi v = F + u, \quad (1)$$

$$\dot{v} + \Lambda v + \kappa \dot{x} = 0, \quad (2)$$

\*All authors are from the Rio de Janeiro State University, Rua São Francisco Xavier, 524 - Maracanã, Rio de Janeiro - RJ, 20550-013.

<sup>1</sup> basilio.julio@posgraduacao.uerj.br

<sup>2</sup> tiagoroux@uerj.br

<sup>3</sup> jose.ribeiro@uerj.br

<sup>4</sup> amercico.cunha@uerj.br

where  $v$  represents the voltage across the resistor,  $x$  is the horizontal displacement of the tip of the beam,  $t$  is the time variable,  $\chi$  is the mechanical coupling factor,  $\kappa$  is the electrical coupling factor,  $\Lambda$  is the inverse characteristic time,  $u$  is the control signal and  $F$  is the natural system excitation, which can be harmonic or random.

The Eq. (1) and Eq. (2) are complemented by the initial conditions  $x(0) = x_0$ ,  $\dot{x}(0) = \dot{x}_0$  and  $v(0) = v_0$ , which depending on their values can result in system trajectories with chaotic behavior [2] [19]. There are even studies that use this system to perform chaos control through the extended delayed feedback method [24] and OGY method [25].

A harvester system with harmonic behavior presents more energy to be harvested. In this context, the purpose of this paper is to control the randomly excited energy harvesting system, through the horizontal displacement of the beam tip  $x$ , to pursue the reference displacement  $x_{ref}$  of the same energy harvesting system harmonically excited by  $F = f \cos(\Omega t)$ .

### III. FRACTIONAL-ORDER SLIDING MODE CONTROL

In any control problem, there is always a difference between the real dynamics of the plant and its mathematical model used in the controller design, either due to internal or external disturbances, lack of knowledge of the plant parameters or due to unmodeled dynamics. To solve this problem, robust methods for control were developed and with them the SMC is one of the most successful approaches in dealing with uncertainties. Its idea is to guide the system trajectory towards a “tailored” designed sliding surface, which is introduced in the controller design by the sliding variable  $S$ . Since the sliding variable is driven to zero, the control signal that is reached on the sliding surface is expected to remain the system trajectories on the surface and slide to the origin point which is the desired position, as illustrated in Fig. 2 [5] [33].

The sliding surface of the SMC control in a second-order system, as presented in section II, can be obtained according to proposed in [5]:

$$S(t) = \lambda_1 e(t) + \frac{d e(t)}{dt} \quad (3)$$

where  $\lambda_1 \in \mathbb{R}$  denotes the sliding gain and  $e(t)$  the tracking error. A fractional version of the SMC, as shown in Eq. (3), is only possible due to the increasing development of the theory of fractional calculus, where many different fractional operators were proposed, including the fractional derivatives of Riemann-Liouville and Caputo [12] [16] [20] [21] [22].

The fractional Riemann-Liouville integral [16] of order  $\alpha$ , where  $\alpha \in \mathbb{R}$  and  $\alpha > 0$ , is defined in terms of a convolution operation between the function of real value  $y(t)$  and kernel  $t^{\alpha-1}$

$$\mathcal{I}_{a,t}^\alpha y(t) = \frac{1}{\Gamma(\alpha)} \int_a^t (t - \tau)^{\alpha-1} y(\tau) d\tau, \quad t > a \quad (4)$$

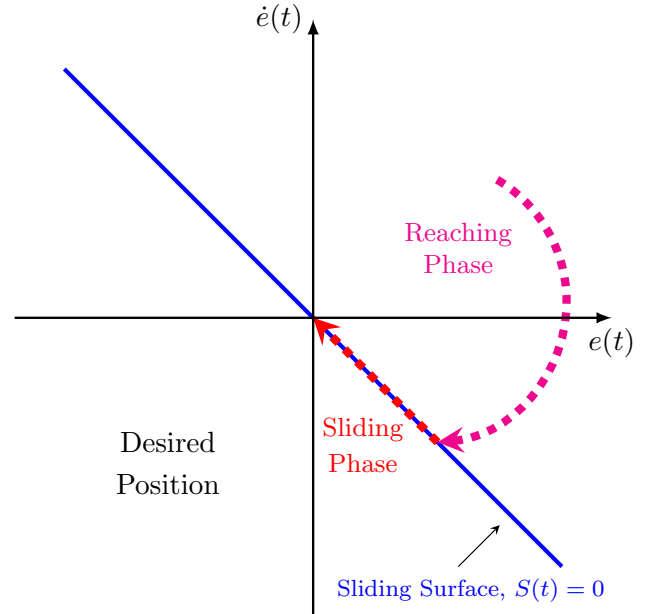


Fig. 2. Schematic representation of the Sliding Mode Control (SMC), where  $e(t)$  and  $\dot{e}(t)$  are the tracking error and its derivative. Adapted from [5].

where  $\Gamma$  is the Gamma function. The fractional Riemann-Liouville derivative [16] is defined in terms of the classical derivative of order  $n \in \mathbb{Z}^+$  and the integral of fractional-order Eq. (4)

$${}_{RL}\mathcal{D}_{a,t}^\alpha y(t) = \frac{1}{\Gamma(n - \alpha)} \frac{d^n}{dx^n} \int_a^t (t - \tau)^{n-\alpha-1} y(\tau) d\tau, \quad (5)$$

is a global operator (not local as in classical calculus) that presents “memory”, with  $t > a$  and  $n-1 < \alpha < n$ . With numerical methods emerged to simulate fractional system, who usually use the fractional derivative of Grünwald-Letnikov [11] [17] [31], was made it possible to implement fractional operators in controllers [3] [6] [23] [30] [32].

The use of the fractional derivative instead of the classical derivative on the sliding surface of Eq. (3) result in an unfeasible control. Therefore, for this paper, the fractional version of the SMC used in simulations is based on the controller designed in [1]. So considering a second order system, the sliding surface of the FOSMC fractional control can be obtained by:

$$S(t) = \lambda_1 e(t) + \lambda_2 \frac{d e(t)}{dt} + \lambda_3 \mathcal{D}^\alpha e(t) \quad (6)$$

where  $\lambda_1$ ,  $\lambda_2$  and  $\lambda_3 \in \mathbb{R}$  are proper sliding gains and  $\mathcal{D}^\alpha$  is the fractional derivative operator.

The general expression for the control signal of both SMC and FOSMC consists of a switching control term and equivalent control term as indicated in Eq. (7)

$$u(t) = u_{eq}(t) + u_{sw}(t) \quad (7)$$

where the switching control  $u_{sw}$  corresponds to the reaching phase when  $S(t) \neq 0$ , while the equivalent control  $u_{eq}$  corresponds to the sliding phase when  $S(t) = 0$ . Both control terms are obtained from the stability analysis by the Lyapunov theorem, as used in [5]. From the following Lyapunov function candidate:

$$V(S) = \frac{1}{2} S^2 \quad (8)$$

where  $V(S) > 0$  and  $V(0) = 0$ , we find  $u(t)$  in Eq. (7) so that the derivative of Eq. (8) must be negative definite, i.e.,

$$\dot{V}(S) = S \dot{S} < 0. \quad (9)$$

Hence, the equivalent control  $u_{eq}$  is set to make  $\dot{V}(S) = 0$  and the switching control  $u_{sw}$  is set to make  $\dot{V}(S) < 0$ , according to the following expression:

$$u_{sw} = -k \frac{S}{||S|| + \epsilon} \quad (10)$$

where  $k$  is the switching control gain that modulates the term that replaces the sign function to avoid chattering from the definition of  $\epsilon > 0$ , which is sufficiently small.

To illustrate the proposed fractional control method (FOSMC), several simulations were performed with different initial conditions for the following academic example:

$$\ddot{y} + \dot{y}^2 \cos(3y) = u \quad (11)$$

where  $y$  is the output variable to be controlled so that it is equal to zero and  $u$  is the control signal. By setting  $k = 100$ ,  $\epsilon = 0.1$ ,  $\lambda_1 = 7$ ,  $\lambda_2 = 25$ ,  $\lambda_3 = 1$  and  $\alpha = 0.1$ , the results for the various initial conditions can be seen in the represented phase-plane in Fig. 3. It is possible to clearly observe the sliding surface by which the curves are attracted.

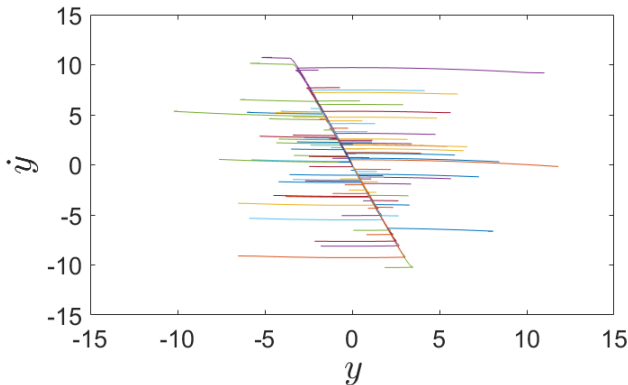


Fig. 3. Phase-plane graph of the academic example controlled by a FOSMC

Now, to obtain the control signal  $u(t)$  of the proposed energy harvester system, both switching  $u_{sw}(t)$  and the equivalent  $u_{eq}(t)$ , it is necessary to define the sliding surface.

The surfaces can be defined from Eq. (3) for the SMC controller and from Eq. (6) for the FOSMC fractional controller, considering the tracking error as

$$e(t) = x(t) - x_{ref}(t) \quad (12)$$

Once the  $S(t)$  sliding surface is defined for both controls, it is enough to take the derivative of the Lyapunov function to obtain the equivalent control signals. Then, substituting the sliding surface of the SMC, given by Eq. (3), in Eq. (9) we have to

$$S (\lambda_1 \dot{e}(t) + \ddot{e}(t)) < 0. \quad (13)$$

Like  $S > 0$ , so

$$\lambda_1 \dot{e}(t) + \ddot{e}(t) < 0 \quad (14)$$

or else

$$\lambda_1 \dot{e}(t) + \ddot{x} - \ddot{r} < 0. \quad (15)$$

Finally, we replace  $\ddot{x}$  with the expression in Eq. (1)

$$\lambda_1 \dot{e}(t) - 2 \xi \dot{x} + \frac{1}{2} x (1 - x^2) + \chi v + F + u - \ddot{r} < 0. \quad (16)$$

Considering  $u = u_{eq} + u_{sw}$  and the switching control signal defined by Eq. (10), therefore the equivalent control signal of the SMC controller  $u_{eq_{IO}}$  can be expressed by

$$u_{eq_{IO}} = \ddot{r} + 2 \xi \dot{x} - \chi v - \frac{1}{2} x (1 - x^2) - F - \lambda_1 \dot{e}. \quad (17)$$

From the same process, but using the sliding surface given by Eq. (6), the equivalent control signal of the FOSMC  $u_{eq_{FO}}$  can be expressed by

$$u_{eq_{FO}} = \ddot{r} + 2 \xi \dot{x} - \chi v - \frac{1}{2} x (1 - x^2) - F - \frac{\lambda_1}{\lambda_2} \dot{e} - \frac{\lambda_3}{\lambda_2} \mathcal{D}^{\alpha+1} e \quad (18)$$

#### IV. CROSS ENTROPY METHOD

The optimal set of controller parameters that result in its optimal performance is the Cross-Entropy method. This method was proposed by R. Rubinstein in 1997 [26] [27] [28] initially for simulation of rare events, and then its effectiveness was observed in the application in optimization problems [14] [29].

Conceptually, the method transforms a non-convex optimization problem into a rare event estimation problem, solved with the aid of a Monte Carlo simulation [9] [14] [15].

The process starts with sampling a viable region according to a given probability distribution  $v_0$ , then the objective function  $\mathcal{F}(X_{1...N^s})$  in each of these samples  $X_{1...N^s}$  is evaluated, including the statistics (mean and standard deviation) that will be used in the adaptation process of the algorithm.

Then, the samples that produced the optimal values for the objective function are identified, this subset is defined as the elite sample set. With this in hand, the parameters of the probability distribution are updated based on the mean and standard deviation of the elite sample set  $\epsilon_t$ , modifying the distribution  $v_t$  to make it as close as possible to a Dirac measure centered at the global optimum. The previous steps are repeated while a stopping criterion, which are dependent on the standard deviation ( $\sigma_t$ ) and mean ( $\mu_t$ ), are not met. This iterative process can be seen in Fig. 4 to follow.

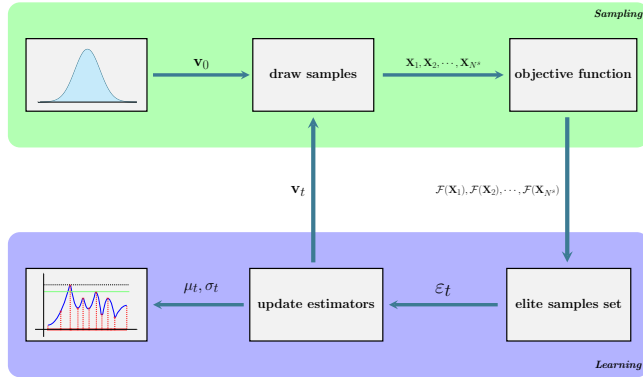


Fig. 4. Schematic representation of the CE algorithm for optimization [8].

For the optimization process performed in this paper, the system performance indicator to compare the two controllers is defined as the ratio between the control effort ( $ISU$ ) and the average power generated ( $P_{avg}$ ) given by the following equations, respectively:

$$ISU = \frac{1}{T} \int_0^T \Lambda u(t)^2 dt \quad (19)$$

$$P_{avg} = \frac{1}{T} \int_0^T \Lambda v(t)^2 dt \quad (20)$$

The ratio  $\mathcal{F} = ISU/P_{avg}$  is the objective function of the optimization process via Cross-Entropy and which one wants to minimize.

## V. RESULTS

The optimization processes to find the ideal parameters of the integer and fractional controllers that result in their best performance were carried out using the Cross-Entropy method code, available in [8], through numerical simulations in Matlab software. For the fractional calculus, the toolbox FOMCON was used for derivatives and integrals of fractional-order [31].

For the simulations reported in this paper, the following values were used both for the system to be controlled (randomly excited) and for the system used as reference (harmonically excited):  $\xi = 0.01$ ,  $\chi = 0.05$ ,  $\kappa = 0.5$  and  $\Lambda = 0.05$ , with initial conditions  $(x_0; \dot{x}_0; v_0) = (1; 0; 0)$ . The parameters of harmonic excitation are given by:  $\Omega = 0.8$  and  $f = 0.2$ . These parameters were chosen because they are known in the literature to result in high energetic values [25].

The results obtained after the optimization of the SMC and FOSMC controllers are presented in Tab. I, with the optimal set of the controllers parameters and their respective performance indexes for each configuration. As can be seen, the FOSMC fractional-order controller reduces up to 93% of the control effort  $ISU$  when compared to the SMC controller, keeping the same amount of average generated power  $P_{avg}$ . The time series of the control signal from both controllers are shown in Fig. 5 showing the reduction in control energy expenditure as well.

TABLE I  
OPTIMIZED PARAMETERS OF SMC AND FOSMC CONTROLLERS AND THEIR RESPECTIVE PERFORMANCE INDEXES.

parameters	SMC	FOSMC
$\epsilon$	0.1	0.1
$k$	13.07	17.27
$\lambda_1$	3.21	11.39
$\lambda_2$	-	0.56
$\lambda_3$	-	10.74
$\alpha$	-	1.65
performance		
$ISU$	378.37	25.11 <b>-93.36%</b>
$P_{avg}$	0.0183	0.0183
$\mathcal{F}$	20697	1374.6

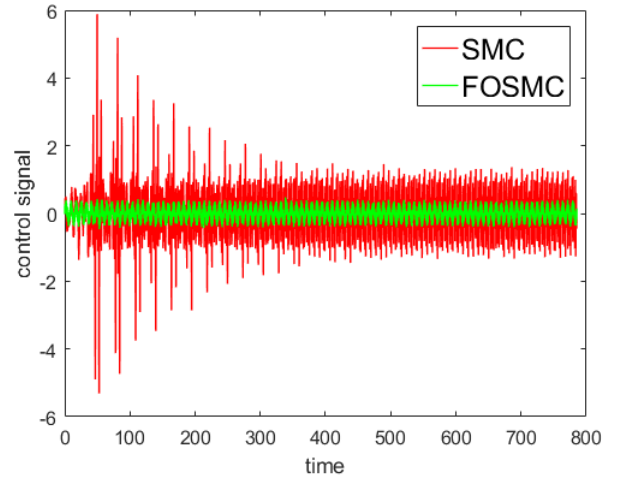


Fig. 5. Time series of SMC and FOSMC control effort.

Finally, Fig. 6 shows a comparison between the phase-plane of the energy harvesting system with the SMC and FOSMC approaches, and also with the reference trajectory. The zoom shows that the fractional controller is more efficient in chasing the reference than the integer controller, that is, it has a smaller tracking error when observed graphically.



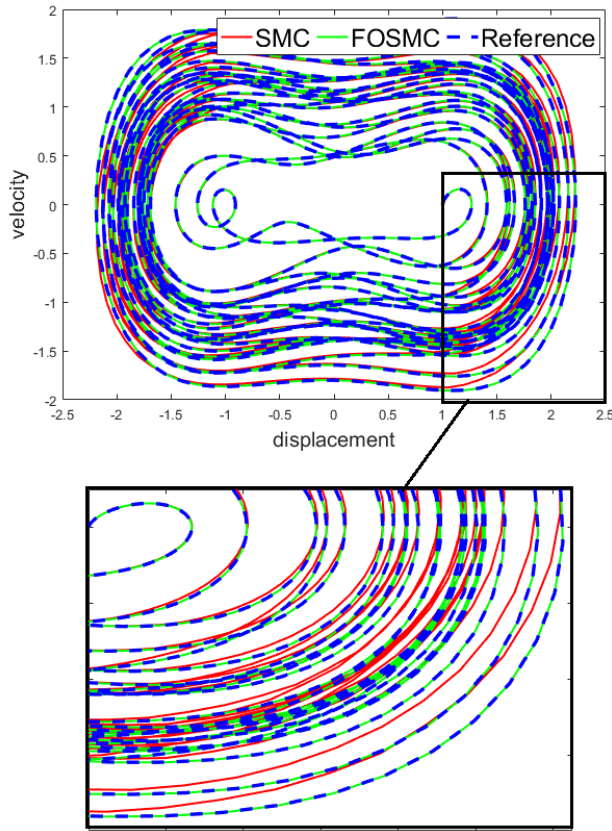


Fig. 6. Phase-plane of reference trajectory and the corresponding responses for SMC and FOSMC controllers.

## VI. CONCLUSION

This paper used an energy harvesting problem to compare the performance of controllers by classical sliding modes (SMC) and fractional-order sliding modes (FOSMC). The objective of the control is to direct the randomly excited system to a trajectory obtained by the same harmonically excited system and with a higher-average power output.

To obtain the ideal configuration of the two types of controllers, the optimization process is carried out via the Cross-Entropy method, aiming to reduce the ratio between the control effort and the average power generated ( $ISU/P_{avg}$ ).

The optimization results indicate that the controller using fractional operators can obtain configurations that reduce the control energy expenditure, making the FOSMC control up to 93% more economical (less control effort), and still maintaining the same generated energy.

In addition, the Cross-Entropy optimization method proved to be effective to find the optimal performance, even with increasing parameters, being a method with potential to deal with fractional controllers.

## ACKNOWLEDGMENT

The authors are grateful for the financial support received from the Brazilian agencies CAPES, CNPq and FAPERJ.

## REFERENCES

- [1] Azar, A.T., Serrano, F.E., Koubaa, A., Ibrahim, H.A., Kamal, N.A., Khamis, A., Ibraheem, I.K., Humaidi, A.J. and Precup, R.E., 2021. Chapter 5 - Robust fractional-order Sliding Mode Control design for UAVs subjected to atmospheric disturbances. In A. Koubaa and A.T. Azar, eds., *Unmanned Aerial Systems*, Academic Press, *Advances in Nonlinear Dynamics and Chaos (ANDC)*, pp. 103–128.
- [2] Barbosa, W., de Paula, A., Savi, M. and Inman, D., 2015. Chaos control applied to piezoelectric vibration-based energy harvesting systems. *The European Physical Journal Special Topics*, Vol. 224, pp. 2787–2801.
- [3] Basilio, J.C., Ribeiro, J.G.T., Cunha, A., Oliveira, T.R. (2022). An Optimal Fractional LQR-Based Control Approach Applied to a Cart-Pendulum System. In: Lacarbonara, W., Balachandran, B., Leamy, M.J., Ma, J., Tenreiro Machado, J.A., Stepan, G. (eds) *Advances in Nonlinear Dynamics*. NODYCON Conference Proceedings Series. Springer, Cham.
- [4] Bingul, Z. and Karahan, O., 2018. Comparison of PID and FOPID controllers tuned by PSO and ABC algorithms for unstable and integrating systems with time delay. *Optimal Control Applications and Methods*, Vol. 39.
- [5] C. C. Soon, R. Ghazali, H. I. Jaafar, and S. Y. S. Hussien, Sliding mode controller design with optimized PID sliding surface using particle swarm algorithm, *Procedia Computer Science*, vol. 105, pp. 235–239, 2017.
- [6] Chen, K., Tang, R., Li, C. and Lu, J., 2018. Fractional order pi controller synthesis for steam turbine speed governing systems. *ISA Transactions*, Vol. 77, pp. 49–57.
- [7] Cottone, F., Vocca, H. and Gammaitoni, L., 2009. Nonlinear energy harvesting. *Physical review letters*, Vol. 102, p. 806.
- [8] Cunha Jr, A. Enhancing the performance of a bistable energy harvesting device via the cross-entropy method. *Nonlinear Dyn* 103, 137–155 (2021).
- [9] Cunha Jr, A, Nasser, R., Sampaio, R., Lopes, H. and Breitman, K., Uncertainty quantification through the Monte Carlo method in a cloud computing setting, *Computer Physics Communications*, v. 185, p. 1355–1363 (2014).
- [10] Delavari, H., Ghaderi, R., Ranjbar, N.A., HosseinNia, S.H. and Mo-mani, S., 2012. Adaptive fractional PID controller for robot manipulator.
- [11] Deng, J., Zhao, L. and Wu, Y., 2015. Efficient algorithms for solving the fractional ordinary differential equations. *Appl. Math. Comput.*, Vol. 269, No. C, p. 196–216.
- [12] D’Elia, M., Gulian, M., Olson, H. et al. Towards a Unified theory of Fractional and Nonlocal Vector Calculus. *Fract Calc Appl Anal* 24, 1301–1355 (2021).
- [13] Erturk, A., Hoffmann, J. and Inman, D.J., 2009. A piezomagnetoelastic structure for broadband vibration energy harvesting. *Applied Physics Letters*, Vol. 94, No. 25, p. 2541.
- [14] Kroese, D.P., Rubinstein, R.Y., Cohen, I., Porotsky, S. and Taimre, T., 2013. *Cross-Entropy Method*, Springer US, Boston, MA, pp. 326–333.
- [15] Kroese, Dirk P., Thomas Taimre, and Zdravko I. Botev. *Handbook of monte carlo methods*. John Wiley & Sons, 2013.
- [16] Li, C. and Deng, W., 2007. Remarks on fractional derivatives. *Applied Mathematics and Computation*, Vol. 187, No. 2, pp. 777–784.
- [17] Li, C., Chen, A. and Ye, J., 2011. Numerical approaches to fractional calculus and fractional ordinary differential equation. *Journal of Computational Physics*, Vol. 230, No. 9, pp. 3352–3368.
- [18] Lin, C.-H.; Hsiao, F.-Y. Proportional-Integral Sliding Mode Control with an Application in the Balance Control of a Two-Wheel Vehicle System. *Appl. Sci.* 2020, 10, 5087.
- [19] Lopes, V.G., Peterson, J.V.L.L. and Cunha Jr., A., 2019. Nonlinear characterization of a bistable energy harvester dynamical system. In M. Belhaq, ed., *Topics in Nonlinear Mechanics and Physics*. Springer Singapore, Singapore, pp. 71–88.
- [20] Machado, J. A. T., Kiryakova, V. and Mainardi, F., Recent history of fractional calculus, *Communications in Nonlinear Science and Numerical Simulation*, 16 (3) (2011) 1140–1153.
- [21] Machado, J.A.T., Galhano, A.M.S.F. and Trujillo, J.J. On development of fractional calculus during the last fifty years. *Scientometrics* 98, 577–582 (2014).
- [22] Ortigueira, M. D., Machado, J. A. T. : What is a fractional derivative? *Journal of Computational Physics*, v. 293, p. 4–13 (2015).

- [23] Ribeiro, J.G.T., Basilio, J.C.C., Cunha Jr, A., Oliveira, T.R. (2021). On the Classical and Fractional Control of a Nonlinear Inverted Cart-Pendulum System: A Comparative Analysis. In: Balthazar, J.M. (eds) *Vibration Engineering and Technology of Machinery. Mechanisms and Machine Science*, vol 95. Springer, Cham.
- [24] Ribeiro, J.G.T., Pereira, M., Cunha, A. et al. Controlling chaos for energy harvesting via digital extended time-delay feedback. *Eur. Phys. J. Spec. Top.* (2022).
- [25] Roca, L., Peterson, J., Pereira, M. and Cunha Jr, A. Control of chaos via OGY method on bistable energy harvester. 25th ABCM International Congress on Mechanical Engineering (COBEM 2019), Oct 2019, Uberlândia, Brazil.
- [26] Rubinstein, R.Y., 1997. Optimization of computer simulation models with rare events. *European Journal of Operational Research*, Vol. 99, No. 1, pp. 89–112.
- [27] Rubinstein, R.Y., 1999. The cross-entropy method for combinatorial and continuous optimization. *Methodology And Computing In Applied Probability*, Vol. 1, pp. 127–190.
- [28] Rubinstein, R.Y. and Kroese, D.P., 2004. The cross-entropy method: a unified approach to combinatorial optimization, Monte-Carlo simulation, and machine learning, Vol. 133. Springer.
- [29] Rubinstein, R.Y. and Kroese, D.P., 2016. *Cross-Entropy Method*, John Wiley Sons, Ltd, chapter 8, pp. 257–306.
- [30] Shah, P. and Agashe, S., 2016. Review of fractional pid controller. *Mechatronics*, Vol. 38, pp. 29–41.
- [31] Tepljakov, A., Petlenkov, E. and Belikov, J., 2011. FOMCOM: a MATLAB toolbox for fractional-order system identification and control. *International Journal of Microelectronics and Computer Science*, Vol. 2, nr 2, pp. 51–62.
- [32] Tepljakov, A., 2017. Fractional-order Modeling and Control of Dynamic Systems.
- [33] Y. Shtessel, C. Edwards, L. Fridman and A. Levant, *Sliding mode control and observation*, New York, NY, USA: Birkhauser, 2014.